Mode locking in driven vortex lattices with transverse ac drive and random pinning

Alejandro B. Kolton,[1] Daniel Domínguez,[1] and Niels Grønbech-Jensen[2,3]
[1]*Centro Atomico Bariloche and Instituto Balseiro, 8400 San Carlos de Bariloche, Rio Negro, Argentina*
[2]*Department of Applied Science, University of California, Davis, California 95616*
[3]*NERSC, Lawrence Berkeley National Laboratory, Berkeley, California 94720*

(Received 20 December 2001; revised manuscript received 19 February 2002; published 22 April 2002)

We find mode-locking steps in simulated current-voltage characteristics of driven vortex lattices with *random* pinning when an applied ac current is *perpendicular* to the dc current. For low frequencies there is mode locking only above a nonzero threshold ac force amplitude, while for large frequencies there is mode locking for any small ac force. This is consistent with the nature of *transverse* temporal order in the different regimes in the absence of an applied ac drive. For large frequencies the magnitude of the fundamental mode-locked step depends linearly on the ac force amplitude.

DOI: 10.1103/PhysRevB.65.184508 PACS number(s): 74.60.Ge, 74.40.+k, 05.70.Fh

Nonlinear dynamics of vortices driven by a current in random media leads to several interesting nonequilibrium phases, such as plastic flow, and moving smectic and moving Bragg glasses.[1–7] These dynamical phases can be characterized by their temporal order[2,4,7–9] and mode-locking responses.[10–13] When a vortex array with average intervortex spacing a is moving at a high enough velocity v, it is possible to have temporal order at the washboard frequency $\omega_0=2\pi v/a$, which results in a peak at ω_0 in the voltage power spectrum.[8,9] This has been observed in numerical simulations[4,13] and also recently in experiments.[8,9] When the system is driven by a dc + ac force with frequency Ω, interference phenomena lead to mode-locking steps for vortex velocities such that $\omega_0=(p/q)\Omega$.[10–13] This interesting effect has been observed experimentally by Fiory[10] and by Harris *et al.*[11] Recently, we have numerically studied how the existence of mode locking in driven vortex lattices depends on the presence of temporal order in each dynamical regime.[13]

Mode-locking phenomena has been extensively studied in other systems in the past, e.g., Josephson junctions (Shapiro steps),[14] Josephson junction arrays,[15] superconductors with periodic pinning,[16–18] and charge-density waves (CDW's).[19,20] Driven vortex lattices with random pinning have two important features that distinguish them from these systems. (i) There is no inherent periodicity, as for example in Josephson-junction arrays and superconductors with periodic pinning. Temporal order and periodicity are induced dynamically due to the vortex-vortex interaction, which tends to favor a structure close to a triangular vortex lattice at large velocities.[2] (ii) The vortex displacements are two-dimensional vectors. This is an important difference with respect to CDW systems where the displacement field is a scalar.[20] In particular, the behavior of the displacements in the direction perpendicular to the driving force shows phenomena such as a transverse critical current[2,4,6] and a transverse freezing transition[2,5] at high velocities. It can therefore be interesting to study the possibility of mode locking when an ac force is applied in the direction *perpendicular* to the direction of the dc driving force. Recently, it has been found in rectangular periodic pinning arrays[18] and in Josephson-junction arrays[21] that a transverse ac force leads to a type of "transverse" phase locking in these cases. In this paper we will investigate the possibility of *transverse mode locking* in driven vortices with random pinning.

The dynamics of a vortex in position $\mathbf{r}_i$ is given by[4,5]

$$\eta\frac{d\mathbf{r}_i}{dt}=-\sum_{j\neq i}\nabla_i U_v(r_{ij})-\sum_p \nabla_i U_p(r_{ip})+\mathbf{F}(t), \quad (1)$$

where $r_{ij}=|\mathbf{r}_i-\mathbf{r}_j|$ is the distance between vortices i,j; $r_{ip}=|\mathbf{r}_i-\mathbf{r}_p|$ is the distance between the vortex i and a pinning site at $\mathbf{r}_p$, $\eta=\Phi_0 H_{c2}d/c^2\rho_n$ is the Bardeen-Stephen friction; and $\mathbf{F}(t)=d\Phi_0/c[\mathbf{J}_{dc}+\mathbf{J}_{ac}\cos(\Omega t)]\times\mathbf{z}$ is the driving force due to an alternating current $\mathbf{J}_{ac}\cos(\Omega t)$ superimposed to a constant current $\mathbf{J}_{dc}$. The vortex-vortex interaction is considered logarithmic: $U_v(r)=-A_v\ln(r/\Lambda)$, with $A_v=\Phi_0^2/8\pi\Lambda$, and $\Lambda=2\lambda^2/d$ is the effective penetration depth of a thin film of thickness d.[5,13] The vortices interact with a random distribution of attractive pinning centers with $U_p(r)=-A_p e^{-(r/\xi)^2}$, ξ being the coherence length. Length is normalized by ξ, energy by A_v, and time by $\tau=\eta\xi^2/A_v$. We consider N_v vortices and N_p pinning centers in a rectangular box of size $L_x\times L_y$, and the normalized vortex density is $n_v=N_v\xi^2/L_xL_y=B\xi^2/\Phi_0$. Moving vortices induce a total electric field $\mathbf{E}=(B/c)\mathbf{v}\times\mathbf{z}$, with $\mathbf{v}=1/N_v\Sigma_i\mathbf{v}_i$.

We study the response of the vortex lattice to a dc force plus a *transverse* ac force, $\mathbf{F}=F_{dc}\mathbf{y}+F_{ac}\cos(\Omega t)\mathbf{x}$ solving Eq. (1) for different values of F_{ac} and Ω. The simulations are at $T=0$ for a vortex density $n_v=0.04$ in a box with $L_x/L_y=\sqrt{3}/2$, and $N_v=64,100,144,196,256,324$, and 400 (we show results for $N_v=256$), and we consider weak pinning strength of $A_p/A_v=0.05$ with a density of pinning centers being $n_p=0.08$. We impose periodic boundary conditions and the long-range interaction is determined by Ref. 22. The time integration step is $\Delta t=0.001\tau$ and averages are evaluated during 131 072 steps after 3000 steps for equilibration.

In a previous work[13] we studied the case of a longitudinal ac force, relating the mode-locking response with the presence of temporal order for the longitudinal component of the velocity. Here we analyze the *transverse temporal order* from the transverse power voltage spectra (corresponding to the transverse velocity), which are shown in the insets of Fig.

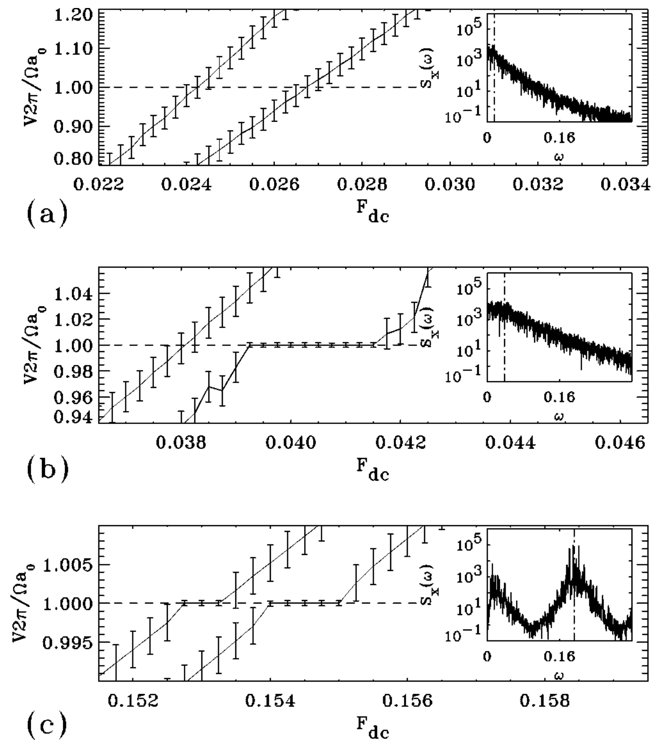

FIG. 1. Velocity-force curve around the main interference condition $V=\Omega a_0/2\pi$ for three typical drive frequencies Ω. Each case shows results for two values of amplitude F_{ac} (the curves are shifted in F_{dc} for clarity). Insets show corresponding voltage power spectrum for $F_{ac}=0$ and $V\approx V_{step}$. Vertical dashed line in the spectral density indicates the expected washboard frequency ω_0. (a) $\Omega=0.02$, $F_{ac}=0.01$ (left), $F_{ac}=0.03$ (right). (b) $\Omega=0.04$, $F_{ac}=0.02$ (left), $F_{ac}=0.08$ (right). (c) $\Omega=0.19$, $F_{ac}=0.09$ (left), $F_{ac}=0.23$ (right).

1. They are calculated as $S_x(\omega)=|1/T\int_0^T dt V_x(t)\exp(i\omega t)|^2$ at the different dynamical regimes for $F_{ac}=0$.[5] The first regime above the critical depinning force F_c is the plastic flow regime ($F_c<F_{dc}<F_p$, $F_c\approx 0.01$, $F_p\approx 0.03$). In this case we find a broad band spectrum without temporal order [inset of Fig. 1(a)]. Similar behavior is found in the "smectic flow" regime ($F_p<F_{dc}<F_t$, $F_t\approx 0.06$), shown in the inset of Fig. 1(b). This is reasonable, since we know that the transverse motion is diffusive in both regimes.[5] Only for $F_{dc}>F_t$, in the "transverse solid" regime, do we find clear evidence of temporal order in the transverse velocity. This is seen in the inset of Fig. 1(c) where well-developed peaks appear at the washboard frequency, ω_0, and its harmonics. We are now ready to study the response to a superimposed transverse ac force $F_{ac}\cos(\Omega t)$, for varying values of F_{ac}. For a given Ω, we expect the main interference step ($p=q=1$) to occur when $V=V_{step}=\Omega a/2\pi$ (i.e., $\Omega=\omega_0$) if there is mode locking. We therefore choose the values of Ω such that the expected step, $V_{step}=\Omega a/2\pi$, would correspond to velocities V belonging to a given dynamical regime of the limit $F_{ac}=0$. Each simulation is started at $\langle v_y\rangle\approx 0.975\Omega a/2\pi$ with an ordered triangular lattice up to values such that $\langle v_y\rangle\approx 1.025\Omega a/2\pi$ by slowly increasing the dc force F_{dc} with $\Delta F_{dc}=0.000\,05-0.000\,25$. We have chosen ΔF_{dc} such that

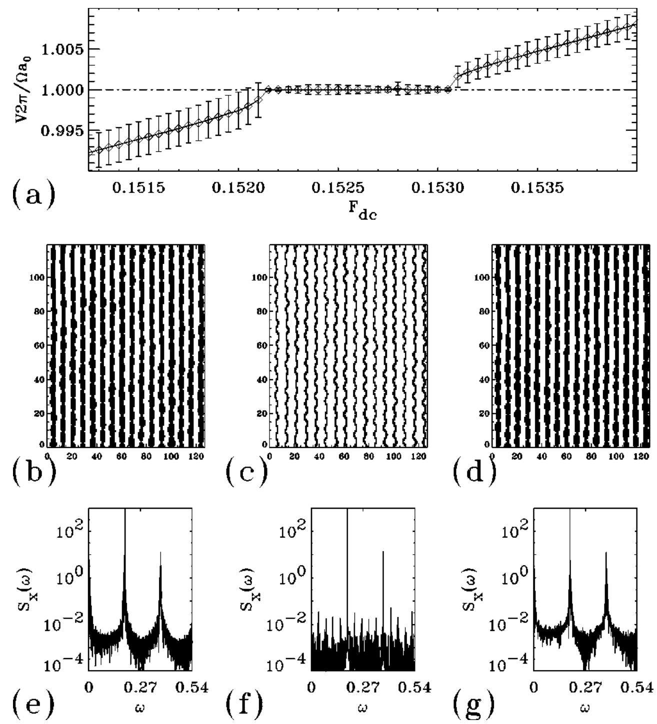

FIG. 2. (a) Velocity-force curve around the main interference step for $\Omega=0.08$ and $F_{ac}=0.3$. (b)–(d) Typical time-averaged coarse-grained densities of vortices for a mode-unlocked state below the step, a mode-locked state in the step, and a mode-unlocked state above the step, respectively. (e)–(g) Typical voltage power spectrum for the three ac-driven regimes mentioned above.

$\Delta F_{dc}/F_c\lesssim 0.01$, which is small enough to obtain a behavior independent of rate of ramping of the dc driving force in all the IV curves. For low Ω, for which we have plastic flow when $F_{ac}\to 0$, we find that there are no interference steps in a wide range of F_{ac} [shown in Fig. 1(a) for $F_{ac}/V_{step}<1$ (left curve) and $F_{ac}/V_{step}>1$ (right curve)]. For intermediate Ω, for which we have smectic flow when $F_{ac}\to 0$, we find that there are no steps for small amplitudes, $F_{ac}/V_{step}<1$, while there are steps for $F_{ac}/V_{step}>1$, as shown in Fig. 1(b) in the left and right curves, respectively. For high Ω, corresponding to a transverse solid regime when $F_{ac}\to 0$, we find that there are steps both for small $F_{ac}/V_{step}<1$ and large $F_{ac}/V_{step}>1$ values of the ac amplitude, as we can observe in Fig. 1(c). We therefore find a behavior similar to the case of longitudinal ac forces.[13] In the present case, when the dynamical regime has transverse temporal order, any small amount of F_{ac} will induce transverse mode locking, while for the dynamical regimes that do not have transverse temporal order, a nonzero (threshold) value of F_{ac} is needed to induce transverse mode locking.

In Fig. 2(a) we show in detail a typical V-F_{dc} curve around the transverse mode-locking step. To visualize the spatial structure of trajectories in the transition we define a coarse-grained vortex density $\rho_v(\mathbf{r},t)$. We take a coarse-graining scale $\Delta r<a_0$. In Figs. 2(b)–2(d) we show the temporal average $\langle\rho_v(\mathbf{r},t)\rangle$ of the density for three typical values of F_{dc}, corresponding to voltages $V<V_{step}$ [Fig. 2(b)], $V=V_{step}$ [Fig. 2(c)], and $V>V_{step}$ [Fig. 2(d)]. We observe in

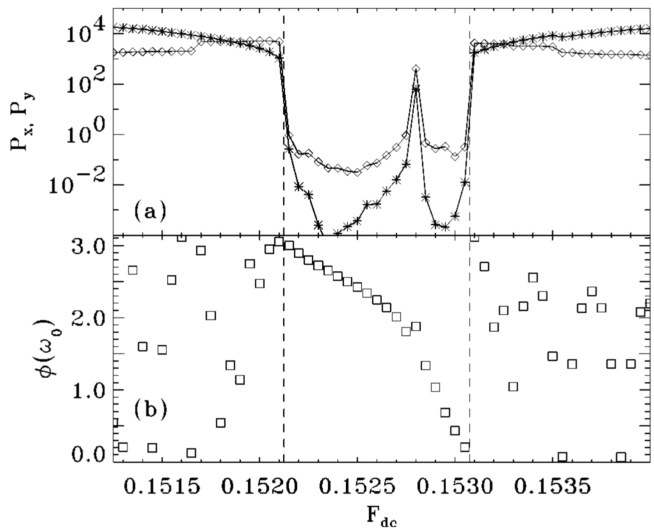

FIG. 3. (a) Low-frequency voltage noise in the transverse and longitudinal directions around the main interference step. The dashed lines indicate the mode-locking transitions. (b) Phase of the washboard frequency component of the longitudinal voltage Fourier transform around the step.

Fig. 2(b) that within the mode-locked state vortices follow one-dimensional trajectories. The wavy nature of the trajectories is, of course, due to the transverse ac force. Figures 2(e)–2(g) show typical transverse voltage spectral densities $S_x(\omega)$ for the three cases mentioned above. We see that there is a significant reduction in the width of the washboard peak within the step, a typical signature of mode locking.[19,20] In Fig. 3(a) we show the low-frequency voltage noise in both directions, perpendicular P_x, and longitudinal P_y to the dc force, defined as $P_{x,y}=\lim_{\omega\to 0}S_{x,y}(\omega)$. We see that also the low-frequency noise is greatly reduced within the step. (There is a noise peak inside the step which corresponds to a transition between different mode-locked structures.) In Fig. 3(b) we show the phase $\phi(\omega_0)$ of the washboard frequency component of the longitudinal voltage Fourier transform $\tilde{V}(\omega_0)$, defined as $\tilde{V}(\omega_0)=\sqrt{S_y(\omega_0)}\exp[i\phi(\omega_0)]$. Here we see explicitly that within the "phase-locked" state there is a well-defined "phase" which varies within the range $0\leqslant\phi\leqslant\pi$. We have checked for finite-size effects by calculating the phase-locking range (step width) ΔF_{dc} for a number of vortices in the range $N_v=64-400$. In Fig. 4 we show the size dependence of the step width ΔF_{dc} for the step corresponding to $F_{ac}=0.2$ and $\Omega=0.19$, where the error bars are due to the observed dependence of the width in three different realizations of disorder. We observe that for $N_v>256$, ΔF_{dc} tends to a size-independent value.

In Fig. 5(a) and 5(b) we show the range (width) ΔF_{dc} for the cases $F_p<F_{dc}<F_t$ and $F_t<F_{dc}$, respectively. The error bars and the mean values were estimated by repeating the simulation for three different disorder realizations. In Fig. 5(a) we show ΔF_{dc} for $\Omega=0.04$ vs F_{ac}, which corresponds to the smectic flow regime for $F_{ac}\to 0$. We see that there is mode locking only above a nonzero threshold value $F_{ac}/V_{step}\approx 1$ [see inset of Fig. 1(a)]. In Fig. 5(b) we show ΔF_{dc} for two frequencies $\Omega=0.13,0.19$ vs F_{ac}, which correspond to the transverse solid in the $F_{ac}=0$ limit. We can collapse (approximately) both curves into a single curve if we plot ΔF_{dc} vs F_{ac}/V_{step}. Our results follow closely a dependence of the form $\Delta F_{dc}\approx A|J_1(F_{ac}/V_{step}\sqrt{3})|$ with A being a constant. In the inset of Fig. 5(b) we can see that there is a linear dependence of the mode locking intensity with F_{ac}. This is very different from transverse mode-locking in periodic pinning systems,[18,21] in which the step width follows $\Delta F_{dc}\propto(F_{ac})^2$. The rather surprising result that in the random pinning case the transverse mode-locking intensity has a linear F_{ac} dependence, can be explained as a consequence of the existence of transverse temporal order in the $F_{ac}=0$ limit. We can show this with a very simple effective model. The moving lattice can be described approximately by an equation of motion for the velocity $\mathbf{v}$ of its center of mass,

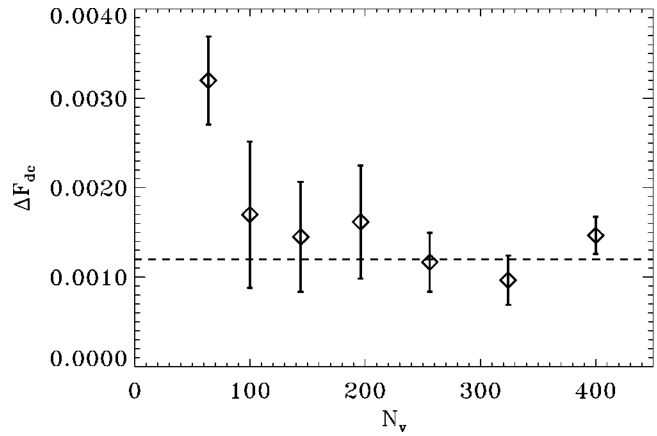

FIG. 4. Dependence of step width ΔF_{dc} with number of vortices N_v, for $F_{ac}=0.2$ and $\Omega=0.19$.

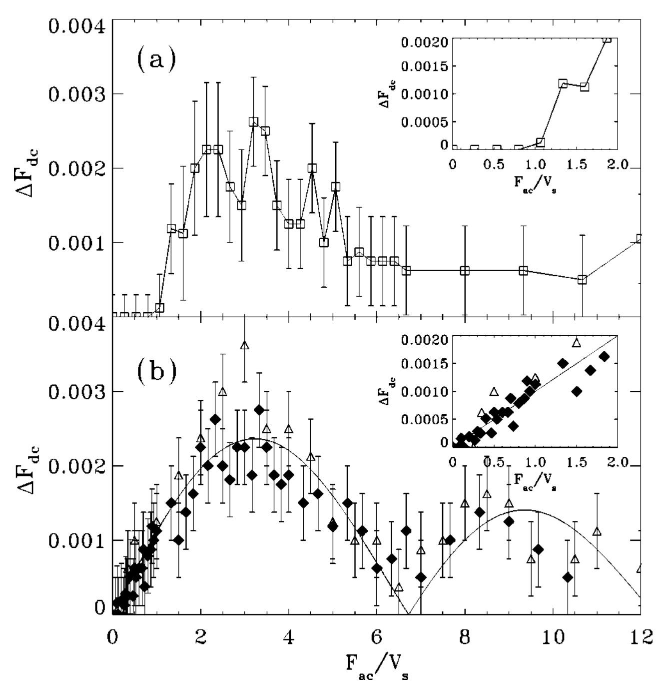

FIG. 5. Step width ΔF_{dc} vs $F_{ac}2\pi/\Omega a_0=F_{ac}/V_{step}$. (a) $\Omega=0.04$. (b) $\Omega=0.13$ ($\triangle$) points and $\Omega=0.19$ [($\diamond$) points]. Solid line shows a fit to $A|J_1(F_{ac}/V_{step}\sqrt{3})|$.

$$\mathbf{v}=\mathbf{F_{dc}}+\mathbf{F_{ac}}\cos(\Omega t)-\sum_{\mathbf{G}}\mathbf{G}U_{\mathbf{G}}\sin(\mathbf{G}\cdot\mathbf{r}). \tag{2}$$

The $U_{\mathbf{G}}$ are the components of an effective periodic force, due to the interaction of the nearly periodic moving lattice (with reciprocal vectors $\mathbf{G}$) with disorder. For weak disorder (small $U_{\mathbf{G}}$) a first-order correction can be obtained assuming that in zero order,

$$\mathbf{r}=\mathbf{r_0}+\langle\mathbf{v}\rangle t+\mathbf{F_{ac}}\sin(\Omega t)/\Omega. \tag{3}$$

This gives for the instantaneous velocity $\mathbf{v}$ and average velocity $\langle\mathbf{v}\rangle$ the following expressions at first order in F_{ac}:

$$\mathbf{v}=\mathbf{F_{dc}}-\sum_{\mathbf{G}}\mathbf{G}U_{\mathbf{G}}\sin[\mathbf{G}\cdot(\mathbf{r_0}+\langle\mathbf{v}\rangle t)]\times\left[J_0\left(\frac{\mathbf{G}\cdot\mathbf{F_{ac}}}{\Omega}\right)+2J_1\left(\frac{\mathbf{G}\cdot\mathbf{F_{ac}}}{\Omega}\right)\sin(\Omega t)\right], \tag{4}$$

$$\langle\mathbf{v}\rangle=\mathbf{F_{dc}}-\sum_{\mathbf{G}}\mathbf{G}U_{\mathbf{G}}\sin(\mathbf{G}\cdot\mathbf{r}_0)\left\{J_0\left(\frac{\mathbf{G}\cdot\mathbf{F_{ac}}}{\Omega}\right)\delta(\mathbf{G}\cdot\langle\mathbf{v}\rangle)-2J_1\left(\frac{\mathbf{G}\cdot\mathbf{F_{ac}}}{\Omega}\right)\delta(\mathbf{G}\cdot\langle\mathbf{v}\rangle-\Omega)\right\}. \tag{5}$$

We consider now an anisotropic triangular lattice with one of its principal axes parallel to $\mathbf{F_{dc}}=\mathbf{y}F_{dc}$, and for simplicity we keep only the shortest reciprocal vectors,

$$\{\mathbf{G}\}=\{\mathbf{g_s},\mathbf{g_l},\mathbf{g_l}-\mathbf{g_s}\}, \tag{6}$$

where

$$\mathbf{g_s}=\mathbf{x}\frac{2\pi}{a_0}\frac{2}{\sqrt{3}},\qquad \mathbf{g_l}=\mathbf{x}\frac{2\pi}{a_0}\frac{1}{\sqrt{3}}+\mathbf{y}\frac{2\pi}{a_0}. \tag{7}$$

Then, we consider

$$U_{\mathbf{g}_l}=U_l=U_{\mathbf{g}_l-\mathbf{g_s}}+\Delta U_l,\qquad U_{\mathbf{g_s}}=U_s. \tag{8}$$

Here ΔU_l represents a small deformation of the perfect triangular lattice such that $\Delta U_l/U_l\ll 1$. U_s and U_l could be related, respectively, to the smectic and longitudinal structure factor peaks of the moving vortex system. Let us first apply this simple model to the longitudinal case $\mathbf{F_{ac}}\|\mathbf{F}_{\mathrm{dc}}$. Writing $\mathbf{F_{ac}}=F_{ac}\mathbf{y}$ we obtain, from Eq. (4), the longitudinal velocity in the limit $F_{ac}=0$,

$$v_y=-\frac{4\pi U_l}{a_0}\sin\left[\frac{2\pi}{a_0}(r_0+\langle v\rangle t)\right]. \tag{9}$$

With this approach we obtain from Eq. (5) the phase-locking range for the first interference step $\Omega=\omega_0$,

$$\Delta F_{dc}=\frac{8\pi|U_l|}{a_0}\left|J_1\left(\frac{\mathbf{g_l}\cdot\mathbf{F}_{ac}}{\Omega}\right)\right|=\frac{8\pi|U_l|}{a_0}\left|J_1\left(\frac{F_{ac}}{V_{\mathrm{step}}}\right)\right|. \tag{10}$$

Even when it was derived for small F_{ac} and small disorder, Eq. (10) corresponds to the relation $\Delta F_{dc}\propto|J_1(F_{ac}/V_{step})|$ found numerically in our previous work in Ref. 13. From Eqs. (9) and (10) we see that, for small F_{ac}, temporal order in the *longitudinal* direction is directly related through U_l with the linear dependence of ΔF_{dc} on F_{ac}. If we apply now the model to the transverse phase-locking case discussed in this paper, with $\mathbf{F_{ac}}=F_{ac}\mathbf{x}$, we obtain for the transverse velocity in the limit $F_{ac}=0$

$$v_x=-\frac{2\pi\Delta U_l}{a_0\sqrt{3}}\sin\left[\frac{2\pi}{a_0}(r_0+\langle v\rangle t)\right] \tag{11}$$

and for the phase-locking range for the first interference step $\Omega=\omega_0$,

$$\Delta F_{dc}=\frac{4\pi|\Delta U_l|}{a_0}\left|J_1\left(\frac{\mathbf{g_l}\cdot\mathbf{F_{ac}}}{\Omega}\right)\right|=\frac{4\pi|\Delta U_l|}{a_0}\left|J_1\left(\frac{F_{ac}}{V_{\mathrm{step}}\sqrt{3}}\right)\right|. \tag{12}$$

We see that Eq. (12) is also the approximate relation found in the simulation, shown in Fig. 5(b). Comparing Eqs. (10) and (12) we see there is a difference by a factor $\sqrt{3}$ in the argument of the Bessel function J_1 in the transverse case with respect to the longitudinal case. Note that this predicted difference is also found numerically, since we obtain $\Delta F_{dc}\propto|J_1(F_{ac}/V_{step}\sqrt{3})|$ in the transverse case shown in Fig. 5(b), and $\Delta F_{dc}\propto|J_1(F_{ac}/V_{step})|$ in Ref. 13. From Eqs. (11) and (12) we see in this case, that, for small F_{ac}, temporal order in the *transverse* direction is directly related through ΔU_l with the linear dependence of ΔF_{dc} on F_{ac}. It is interesting to note that in the perfectly periodic case, $\Delta U_l=0$ and $U_l\neq 0$, there is "longitudinal temporal order" but no "transverse temporal order." Thus the mode-locked step widths would be linear in F_{ac} when $\mathbf{F_{ac}}\|\mathbf{F_{ac}}$ and quadratic in F_{ac} when $\mathbf{F_{ac}}\perp\mathbf{F_{ac}}$. This is because in the perfectly periodic case vortices would move in straight lines without any transverse component of the velocity, and transverse mode locking would arise as a second-order effect. In conclusion, a small amount of lattice distortion is enough to induce transverse temporal order, and, thus, a linear step width dependence with F_{ac}.

We acknowledge discussions with V. I. Marconi and C. Reichhardt. This work has been supported by CONICET, CNEA, and ANPCYT PICT99-03-06343 (Argentina) and by the Director, Office of Advanced Scientific Computing Research, Division of Mathematical, Information, and Computational Sciences of the U.S. Department of Energy (Contract No. DE-AC03-76SF00098).

[1] H. J. Jensen, A. Brass, and A. J. Berlinsky, Phys. Rev. Lett. **60**, 1676 (1988); A.-C. Shi and A. J. Berlinsky, *ibid.* **67**, 1926 (1991).
[2] A. E. Koshelev and V. M. Vinokur, Phys. Rev. Lett. **73**, 3580 (1994); S. Scheidl and V. M. Vinokur, Phys. Rev. B **57**, 13 800 (1998); T. Giamarchi and P. Le Doussal, Phys. Rev. Lett. **76**, 3408 (1996); P. Le Doussal and T. Giamarchi, Phys. Rev. B **57**, 11 356 (1998); L. Balents, M. C. Marchetti, and L. Radzihovsky, *ibid.* **57**, 7705 (1998).
[3] F. Pardo, F. de la Cruz, P. L. Gammel, E. Bucher, and D. J. Bishop, Nature (London) **396**, 348 (1998).
[4] K. Moon, R. T. Scalettar, and G. T. Zimányi, Phys. Rev. Lett. **77**, 2778 (1996); S. Ryu, M. Hellerqvist, S. Doniach, A. Kapitulnik, and D. Stroud, *ibid.* **77**, 5114 (1996); N. Grønbech-Jensen, A. R. Bishop, and D. Domínguez, *ibid.* **76**, 2985 (1996); C. Reichhardt, C. J. Olson, and F. Nori, *ibid.* **78**, 2648 (1997); D. Domínguez, Niels Grønbech-Jensen, and A. R. Bishop, *ibid.* **78**, 2644 (1997); C. J. Olson, C. Reichhardt, and F. Nori, *ibid.* **81**, 3757 (1998); D. Domínguez, *ibid.* **82**, 181 (1999); H. Fangohr, S. J. Cox, and P. A. J. de Groot, Phys. Rev. B **64**, 064505 (2001); K. E. Bassler, M. Paczuski, and E. Altshuler, *ibid.* **64**, 224517 (2001).
[5] A. B. Kolton, D. Domínguez, and Niels Grønbech-Jensen, Phys. Rev. Lett. **83**, 3061 (1999); A. B. Kolton, D. Domínguez, C. J. Olson, and Niels Grønbech-Jensen, Phys. Rev. B **62**, R14 657 (2000).
[6] C. J. Olson and C. Reichhardt, Phys. Rev. B **61**, R3811 (2000); H. Fangohr, P. A. J. de Groot, and S. J. Cox, *ibid.* **63**, 064501 (2001).
[7] L. Balents and M. P. A. Fisher, Phys. Rev. Lett. **75**, 4270 (1995).
[8] A. M. Troyanovski, J. Aarts, and P. H. Kes, Nature (London) **399**, 665 (1999).
[9] Y. Togawa, R. Abiru, K. Iwaya, H. Kitano, and A. Maeda, Phys. Rev. Lett. **85**, 3716 (2000).
[10] A. T. Fiory, Phys. Rev. Lett. **27**, 501 (1971); Phys. Rev. B **7**, 1881 (1973); *ibid.* **8**, 5039 (1973).
[11] J. M. Harris, N. P. Ong, R. Gagnon, and L. Taillefer, Phys. Rev. Lett. **74**, 3684 (1994).
[12] A. Schmid and W. Hauger, J. Low Temp. Phys. **11**, 667 (1973); J. Müllers and A. Schmid, Phys. Rev. Lett. **75**, 136 (1995); A. I. Larkin and Yu. N. Ovchinikov, Zh. Éksp. Teor. Fiz. **65**, 1704 (1973) [Sov. Phys. JETP **38**, 854 (1974)].
[13] A. B. Kolton, D. Domínguez, and Niels Grønbech-Jensen, Phys. Rev. Lett. **86**, 4112 (2001); **88**, 079902(E) (2002).
[14] S. Shapiro, Phys. Rev. Lett. **11**, 80 (1963); A. Barone and G. Paterno, *Physics and Applications of the Josephson Effect* (Wiley, New York, 1982).
[15] S. P. Benz, M. S. Rzchowski, M. Tinkham, and C. J. Lobb, Phys. Rev. Lett. **64**, 693 (1990); K. H. Lee, D. Stroud, and J. S. Chung, *ibid.* **64**, 962 (1990); D. Domínguez and J. V. José, *ibid.* **69**, 514 (1992); Int. J. Mod. Phys. B **8**, 3749 (1994).
[16] P. Martinoli, O. Daldina, C. Leemann, and E. Stocker, Solid State Commun. **17**, 207 (1975); L. Van Look, E. Rosseel, M. J. Van Bael, K. Temst, V. V. Moshchalkov, and Y. Bruynseraede, Phys. Rev. B **60**, R6998 (1999).
[17] C. Reichhardt, R. T. Scalettar, G. T. Zimányi, and Niels Grønbech-Jensen, Phys. Rev. B **61**, R11 914 (2000).
[18] C. Reichhardt, A. B. Kolton, D. Domínguez, and N. Grønbech-Jensen, Phys. Rev. B **64**, 134508 (2001).
[19] G. Grüner, Rev. Mod. Phys. **60**, 1129 (1988); S. Bhattacharya, J. P. Stokes, M. J. Higgins, and R. A. Klemm, Phys. Rev. Lett. **59**, 1849 (1987); M. J. Higgins, A. A. Middleton, and S. Bhattacharya, *ibid.* **70**, 3784 (1993).
[20] L. Sneddon, M. C. Cross, and D. S. Fisher, Phys. Rev. Lett. **49**, 292 (1982); S. N. Coppersmith and P. B. Littlewood, *ibid.* **57**, 1927 (1986); A. A. Middleton, O. Biham, P. B. Littlewood, and P. Sibani, *ibid.* **68**, 1586 (1992).
[21] V. I. Marconi, A. B. Kolton, D. Domínguez, and N. Grønbech-Jensen (unpublished).
[22] N. Grønbech-Jensen, Int. J. Mod. Phys. C **7**, 873 (1996); Comput. Phys. Commun. **119**, 115 (1999).